Execution technique and pigment characteristics of the decorative wall from seventeenth-century CE Chatta Chowk at Red Fort Complex, New Delhi, India

Anjali Sharma [1] and Manager Rajdeo Singh [2,*]

[1] Department of Conservation, National Museum Institute, New Delhi, India-110011
[2] National Research Laboratory for Conservation of Cultural Property, E-3/Aliganj, Lucknow, India-226024

ARTICLE INFO

ABSTRACT

The decorative wall painting from seventeenth-century CE Chatta Chowk at Red Fort Complex was investigated to study the composition and characteristics of the pigment used in the decorative arts. The pigments were examined by thin cross-sections, High-Resolution X-ray diffraction (HR-XRD) analysis, Fourier-transform infrared spectroscopy (FTIR), and portable Raman spectrometry. Besides, gas chromatograph-mass spectrometry (GC-MS) was used for identifying pigment binders. Analytical results showed the stratigraphy of the paint layer applied over fine lime plaster in well-controlled mixing with binders according to the secco technique. The identified pigments for red paint layers were attributed to the mixture of hematite (Fe_2O_3), cinnabar (HgS) and cadmium sulfide (CdS). The utilization of a mixture of mercury, iron, and cadmium compounds has served as a clear evidence in order to specific tones on the painted surfaces. The green paint layer was attributed to green earth (celadonite) through vibrational features, differentiating from glauconite spectra. The GC-MS analysis of the pigment showed the use of fats, waxes, and drying oils as binders.

Keywords: Pigments; Decorative arts; Paint layer; Binders; Cinnabar; Celadonite.

INTRODUCTION

The pigments of decorative wall paintings from seventeenth-century CE at Chatta Chowk at Red Fort Complex, New Delhi (Figure 1) provides an excellent study to analyze the composition and common technological background that illustrate different levels of technological transfer, change, and innovation. Knowledge and accurate identification of various constituents of the pigment are crucial for their appropriate conservation intervention.

Chatta Chowk (covered bazaar) is one of a long passageway that contains a market and situated behind the Lahori Gate. It is set within an arched passage and fixed with two-story flats that contain 32 arched inlets filling in as shops (Figure 2). During Shah Jahan's rule, the Chatta Chowk was exclusive selective; focusing on exchanging products, for example, silk, brocades, velvet, gold, flatware, gems, diamonds, and valuable stones, to suit the lavish tastes of magnificent family units. It is a unique model of Mughal architecture in which bazaars were commonly open-air. All things considered, the bazaar was once in the past known as Bazaar-I-Musaqaf, with a saqaf, signifying "rooftop" (Sanyal, 2008).

The decorative wall is the most important piece of the historical building since ancient times. There is particularly fresco and secco technique for the execution of pigment on the lime plaster layer. Pigments are applied onto wet plaster and fixed during the carbonization of lime in the fresco. Whereas in secco they are applied on dry plaster with binders (Agrawal and Pathak, 2001).

Numerous pigments were acquired from inorganic sources such as minerals and organic materials like dyes (*Prehistoric pigments*, n.d.). Natural and mineral pigments such as charcoal and carbon black for black, azurite and rarely lapis lazuli for blue, green earth, and terreverte or
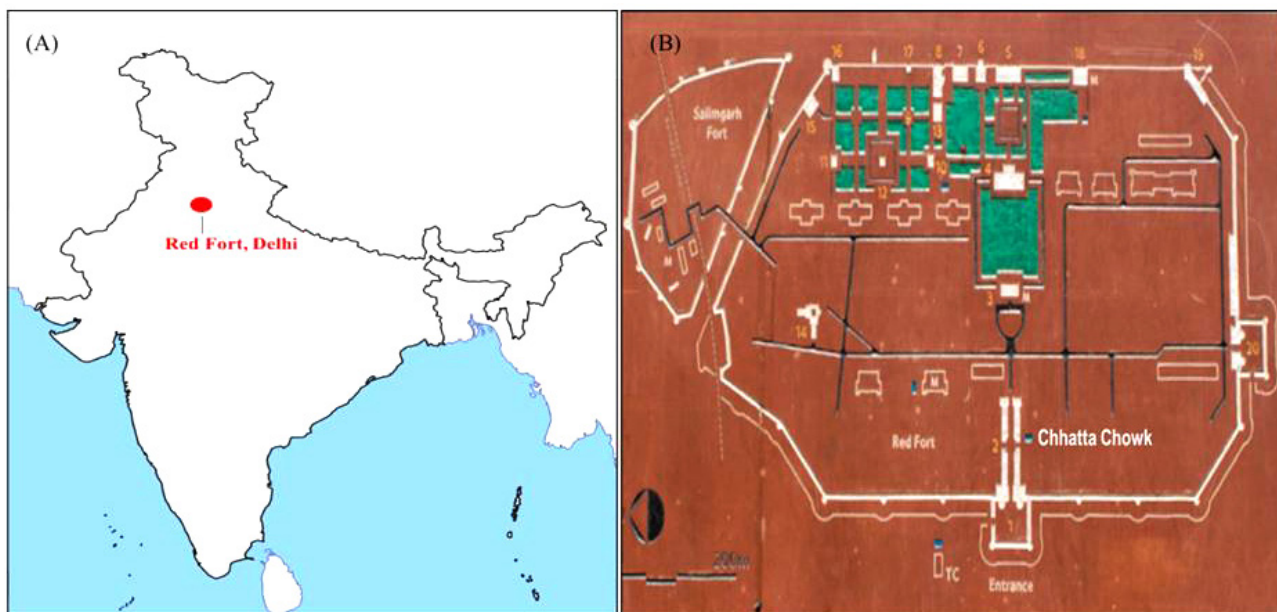
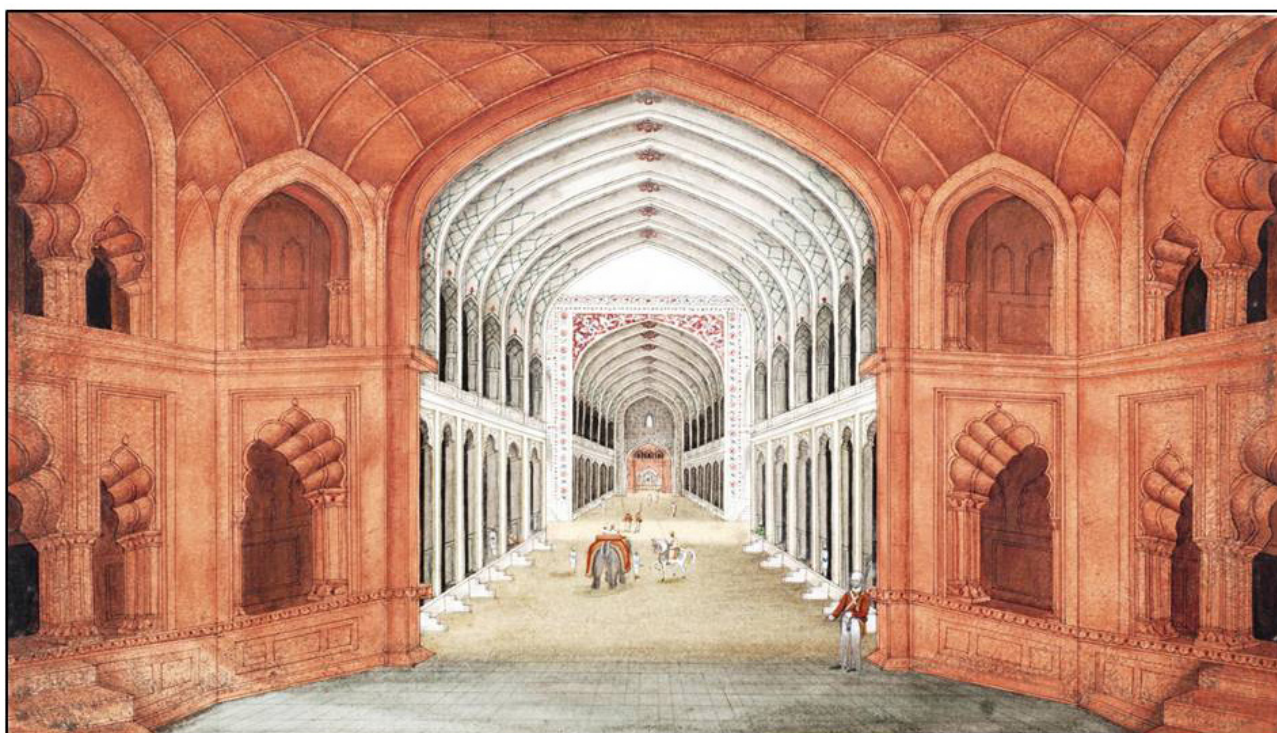Figure 1. (A) Location of Red Fort, Delhi (B) showing map of Chatta Chowk in Red Fort Complex.

Figure 2. Drawing of the Chatta Chowk showing arched bays serving as shops. (Courtesy httpscommons.wikimedia.orgwikiFileGhulam_ Ali_Khan_005b.jpg).

malachite for green, calcite or crushed shells, mineral forms of calcium(II) carbonate ($CaCO_3$) for white, iron oxides, caput mortuum, cinnabar, minium, and umber for reddish-brown, were mostly used in decorative works (Demir et al., 2018).

Nowadays, instrumental and physiochemical techniques have been widely used to examine the availability at a regional and local scale with a view for better

understanding of ancient pigment preparation, techniques and their use (Marcaida et al., 2018). Determining the crystalline phase, elemental composition and, in general, providing sufficient characterization of pigments in cultural arts, the usual techniques have been Optical Microscopy, Fourier Transform Infrared Spectroscopy, Raman Spectroscopy, Scanning Electron Microscopy equipped with EDS microanalysis detector, X-ray Powder Diffraction, Proton-induced X-ray Emission, and X-ray Fluorescence. Analytical pyrolysis coupled with gas chromatography and mass spectrometry is another powerful tool for analyzing binder in the pigment, which also identifies specific pyrolytic profiles and molecular markers (Janssens et al., 2017). The scientific study of pigments is very important for increasing the knowledge about a particular culture and civilization, especially in art history and conservation perspectives (Marcaida et al., 2018). Nonetheless, the assignation of the natural or artificial (synthetic) character of pigments has been a standout amongst the most scientific studies that have been talked about in the logical examinations in the cultural heritage field (Franquelo and Perez-Rodriguez, 2016).

Normally paint surfaces comprise a few complex multilayer's which can be altered due to various degradation factors (natural or anthropogenic sources). The disintegration depends either on the artistic creations encompassing conditions or on the idea of the cooperation between the establishing parts. Identifying pigments and different materials utilized in the making of the compositions is essential so as to gain data with respect to their provenance, creator's artwork–style and techniques or date of generation. All these data are of significance in choosing the most suitable materials and techniques for the fine art's future reclamation (Rusu et al., 2016).

A non-destructive methodology and the utilization of portable instruments for determining the mineralogical composition of pigments, ought to be required when countless samples must be examined or when the investigation alludes with very much safeguarded fine arts that can't be moved, due to they are aesthetic and authentic esteem, to the research facilities (Romano et al., 2011). The two decorative wall fragments involved in the present work were extracted from the Chatta Bazaar ground level. They were subjected to High-Resolution X-ray diffraction (HR-XRD) analysis, Fourier-transform infrared spectroscopy (FTIR) and gas chromatography/ mass spectrometry (GC-MS) experiments were performed to determine the composition and binding media of the pigments. The scanning electron microscope (SEM) analyses coupled with electron dispersive X-ray (EDX) for image analyses and semi-quantitative elemental analyses were used in the present investigations.

Nevertheless, the investigation of the molecular nature of pigments, necessary for their unambiguous identification, performed by means of a portable Raman spectrometer. The analytical analysis provided a variety of data for the morphological, compositional and molecular information of decorative wall fragments.

MATERIALS AND METHODS
Sample description
In this paper, specimens studied were two fragments containing representatives' samples of the pigments used to decorate Chatta Chowk wall in 17th CE Mughal arts. Specimen 1 exhibited three distinctly layered containing colored zones in slightly orange, red and deep red whereas specimen 2 exhibited only single-layered containing green-colored zone. Both specimens (approximately 0.9 mm to 2.1 mm thick pigment layer) were supported with a white base on rough plaster. The specimens dated from the 17th century CE at Chatta Chowk were marked as RP(I), RP(II), RP(III), GP, RL(I), RL(II), RL(III) and GL as shown in Figure 3.

Thin section
A thin section was prepared by placing a sample into plastic molding boxes of 1.5x3x1cm. They were saturated with the polyester mixed with accelerator and hardener under the vacuum of 100 torr. Following their hardening, the molded sample was removed from boxes and cut into the 1mm slice to be fixed and reduced to 25μ thickness on microscope slides (Caner, 2003). The thin section of the sample was examined using FEI Quanta 200 F SEM Field Emission Scanning Electron Microscope (FESEM) at 100x magnification to determine the execution technique.

Analytical methods
High resolution XRD
RigakuSmartLab X-ray diffractometer was used to identify the phases of pigment samples. The pigment and plaster samples were directly mounted on a gonimeter (>500 mm diameter) and operated in Bragg-Brentano geometry equipped with X-Ray tube (anode-Cu sealed, ceramic insulation, 0.4 mm focal spot and operating power of 1.5-2.0 KW). The SmartLab diffractometer features the highest flux X-ray source, HyPix-3000 high energy resolution 2D detector, and new CBO family, with fully automated beam switchable CBO-Auto and high-resolution micro area CBO-μ. The instrument requires a power of 230 VAC single phase or 440V three phases, 50 Hz [15]. The XRD data were analyzed for the identification of mineral phases using Rigaku Software and ICDD PDF4 database.

Figure 3. Fragments from the decorative wall of Chhatta Chowk, where RP(I) red first pigment layer, RP(II) red second pigment layer, RP(III) red third pigment layer, RL(I) first plaster layer of RP(I), RL(II) secon.

High resolution FTIR

The samples were subjected to the Fourier-transformed infrared spectroscopy (FTIR) spectra obtained on a VERTEX 70v vacuum FTIR spectrometer with a diamond single bounce ATR accessory. For each sample, 64 scans were recorded in the mid-IR spectral region (4000-400 cm^{-1}) in the reflectance mode with a 4 cm^{-1} resolution. This spectrometer uses the five beam exit ports on the right, front (fiber optics coupling) and left side (HYPERION IR microscope) and two beam input ports on the right (RAM II FT-Raman module) and rear side (Hg-arc source) of the evacuable optics bench. The DigiTectTM technology prevents the external signal disturbance and guarantees the highest signal-to-noise ratio. Spectral data were collected with the ParaVision 360 software to determine spectroscopic acquisition and data processing.

Portable Raman Spectroscopy

Raman spectra were acquired with a BRAVO handheld Raman spectrometer using sequentially shifted excitation to measure a much wider range of pigments. BRAVO (*Bruker Raman Verification Optics)* features Duo LASER excitation with two wavelengths resulting in high sensitivity across the entire spectral range (300 cm^{-1} to 3200 cm^{-1}), an automated wavenumber calibration for

highly precise measurements, and automated measuring tip recognition IntelliTip. The acquisition time of a spectrum of a material to be stored in a library is identical to the one of verification in the standard measurement mode. OPUS spectroscopy software is used for evaluating data like interpretation and quantification.

SEM-EDX

Morphological observations and elemental analysis were carried out to provide complementary information. The pigment pieces of about 0.80 cm dimensions with at least one flat surface were prepared and subjected to sputter coating with gold under high vacuum for enabling the investigation of conductive, non-conductive and high-vacuum incompatible materials. FEI Quanta 200F SEM Field Emission Scanning Electron Microscope (FESEM) was operated with Oxford-EDX system IE 250 X Max 80 (Netherland) to acquire images through ETD (Everhart-Thornley detector), Backscattered Electrons Detector (BSED), Large Field Detector (LFD), and Gaseous Secondary Electron Detector (GSED). Electron accelerating voltage was set at 15 kiloelectron volt to ensure the generation of X-rays while a beam current of 1 nA (electrostatic unit) with a few percents dead time. SEM micrographs were taken where possible and elemental

analyses were carried out to evaluate together with the micrographs and controlled using Zeiss SmartSEM software while the EDS spectra were collected and analyzed using Bruker Esprit 1.9.4 software.

GC-MS

The pigments were characterized by the presence of organic additives. The selected homogenized sample (80 milligrams) was dissolved in 80 milliliters of methanol (HPLC grade) Sigma-Aldrich at 27 °C for 24 hours. The sample was then filtered using Whatman filter paper (Grade 1). The filtered sample was analyzed using GCMS-QP2010 Ultra instrument (Shimadzu, Kyoto, Japan), equipped with an AOC-5000 plus autosampler an OPTIC-4 injection system and a nonpolar Restek Rxi-5 Sil MS column (5% diphenyl- 95% dimethylpolysiloxane, 30 meters x 0.250-millimeter i.d., x 0.25-micron film thickness). Helium (99.999% Linde) was used as the carrier gas with a flow rate of 0.9 millimeters per minute. Split injection mode at 260 °C with split ration 10.0 and sample volume 1.5 microliter was employed. The column temperature was held at 60 °C for 2 minutes, ramped at 10 °C per minute to 280 °C for 18 minutes (Total run time was 55 minutes). The mass spectrometer was operated with electron impact ionization (70 electronvolts) and in the SCAN monitoring.

Interpretation of GC-MS chromatogram was conducted using the database of National Institute Standard and Technology (NIST) and Wiley having in excess of 62000 patterns. The spectrum of the unknown component was compared with the spectrum of the known components stored in either of the libraries.

RESULTS

Pigments in the two specimens from the fragmented decorative wall at Chatta Chowk, Red Fort were studied by examining their colors (red and green) and fine plaster layer. The detailed description of analytical methods, detected minerals and pigment are mentioned in Table 1.

Painting technique

The thin section examination of the sample RP(I) and GP under the optical microscope enabled us to understand the stratigraphy of the paint layer. The microphotographs confirm the layer sequence shown in Figure 4; the pigment layer, fine plaster layer and rough plaster layer are indicated. The execution techniques of the paintings were identified by examining the border lines (binding medium) between fine plaster and pigment layers. Examined borderlines showed that the pigments were mixed with binders and then applied on dry plaster surfaces by secco technique (Demir et al., 2018).

Characteristics of fine plaster layer

From SEM-EDX results (Table 2), the presence of calcium as the main component of all samples besides the traces of silicon, magnesium, and aluminum, was observed denoting the use of calcium as a binder in the preparation of the plaster base layer.

The mineralogical composition of intonaco layer RL(I)) was indicated by X-ray Diffraction (XRD) and Raman (Şerifaki et al., 2009). In the XRD pattern of the RL(I), calcite and quartz peaks were observed (Figure 5). In its Raman spectrum, calcite bands at 281, 713 and 1086 cm^{-1}, indicated that the fine plaster layer was mainly composed

Table 1. List of samples, analyses performed, and identified minerals and pigments.

| Sample code	Observed Color	Technique used	Detected Mineral or pigment
RP(I)	Slightly orange	OM, HR-XRD, FTIR, p-Raman and SEM-EDX	Cinnabar + Hematite + Cadmium sulfide + Clay
RP(II)	Red	HR-XRD, FTIR, p-Raman and SEM-EDX	Cinnabar + Hematite + Cadmium sulfide + Clay
RP(III)	Red	HR-XRD, FTIR, p-Raman, SEM-EDX and GC-MS	Cinnabar + Hematite + Cadmium sulfide + Clay
GP	Green	OM, HR-XRD, FTIR, p-Raman, SEM-EDX and GC-MS	Green ochre (celadonite) + Iron mica + Calcite + Quartz
RL(I)	Slightly yellowish	HR-XRD, p-Raman, SEM-EDX	Calcite
RL(II)	White	SEM-EDX	Calcite
RL(III)	White	SEM-EDX	Calcite
GL	White	SEM-EDX	Calcite

PM
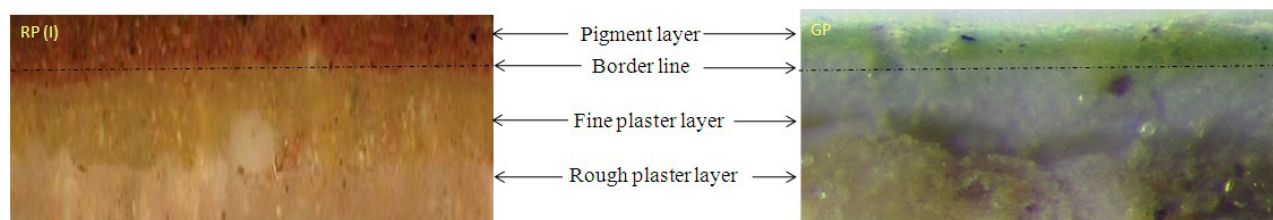
Figure 4. Microphotographs of cross-section of RP(I) and GP samples.

Table 2. Chemical composition (wt%) of pigments and plasters by SEM-EDX.

Element	O	Si	Fe	Al	Ca	C	Mg	S	K	Na	Hg	Cd	Ti
RP(I)	43.23	5.26	9.61	2.31	13.89	4.09	1.68	3.40	0.17	0.73	11.40	4.23	-
RP(II)	45.21	2.09	11.43	0.86	14.13	1.59	0.94	8.36	0.09	0.08	11.59	3.63	-
RP(III)	37.26	12.19	10.12	6.12	6.37	1.81	3.64	2.08	1.05	1.16	15.29	2.82	0.09
Element	O	Ca	Si	Fe	Mg	C	K	Al	S	Cr	Zn	-	-
GP	51.95	13.19	11.36	6.07	4.75	3.33	4.12	2.88	1.00	0.88	0.47	-	-
Element	O	C	Ca	Mg	Na	Si	Al	Mn	S	Hg	-	-	-
RL(I)	53.82	24.15	16.20	1.62	1.12	1.31	0.21	0.95	0.53	0.09	-	-	-
RL(II)	52.34	25.92	15.89	0.96	1.57	0.91	0.89	-	1.52	-	-	-	-
RL(III)	53.67	25.62	16.65	1.20	0.98	0.78	0.87	-	0.23	-	-	-	-
GL	52.82	26.15	16.45	1.35	1.01	1.67	0.21	0.08	0.21	-	-	-	-

of calcium carbonate. This stated that the fine plaster layer was a mixture of calcite and calcium hydroxide (slaked lime), which was then transferred to calcium carbonate by reaction with atmospheric carbon dioxide (Karimy and Holakooei, 2015; Mateos et al., 2015). The first plaster layer RL(I)) has slightly acquired yellowish probably due to a migration of some color pigments into the porous lime layer. However, the other two plaster layer RL(II) and RL(III) were white in color.

In specimen 1, the second pigment layer was laid on the first pigment layer and then the third pigment layer on it. The decorative intonaco layers RL(I), RL(II), RL(III) and GL were found to be fine plasters based on lime with the smooth surface and their thickness range varying from 1 to 1.5 cm.

The SEM-EDS data are in good agreement with the XRD and Raman analysis results of the plasters.

Characteristics of paint layers

Mineralogical and chemical compositions of the paint layers (pigment) were determined by XRD, FT-IR, Raman, and SEM-EDS analyses.

Red colored paint layers

The SEM-EDX results (Table 2) clearly displayed the higher amount of mercury pointing its use as constituents in all three-sample followed by the addition of red ochre and cadmium sulfide to change the hue of red color. The presence of a higher quantity of mercury in the sample was assigned to intense red color. Comparing the color of the sample among three pigment layers RP(I-III), the first pigment layer (RP (I)) is lighter in color (slightly orange) which can be explained by the weight percentage (wt%) of mercury and cadmium in the sample. The wt% of mercury in sample RP (I) is 11.40 as compared to cadmium is 4.34. Although cadmium sulfide is yellow, the presence of mercury in the sample changes the color to slightly orange. However, comparing the percentage of mercury with iron, its mixture doesn't affect the color change of the sample as both colors are assigned red (Fiedler and Bayard, n.d.; Gettens et al., 1993).

EDX data showed the associations of S and Hg with grains containing Si, Al, Mg, Fe, K, O and Ca, typical for chemical compositions of clay minerals and calcite, together with Raman peaks of calcite and silicates observed clearly indicated the natural origin for red
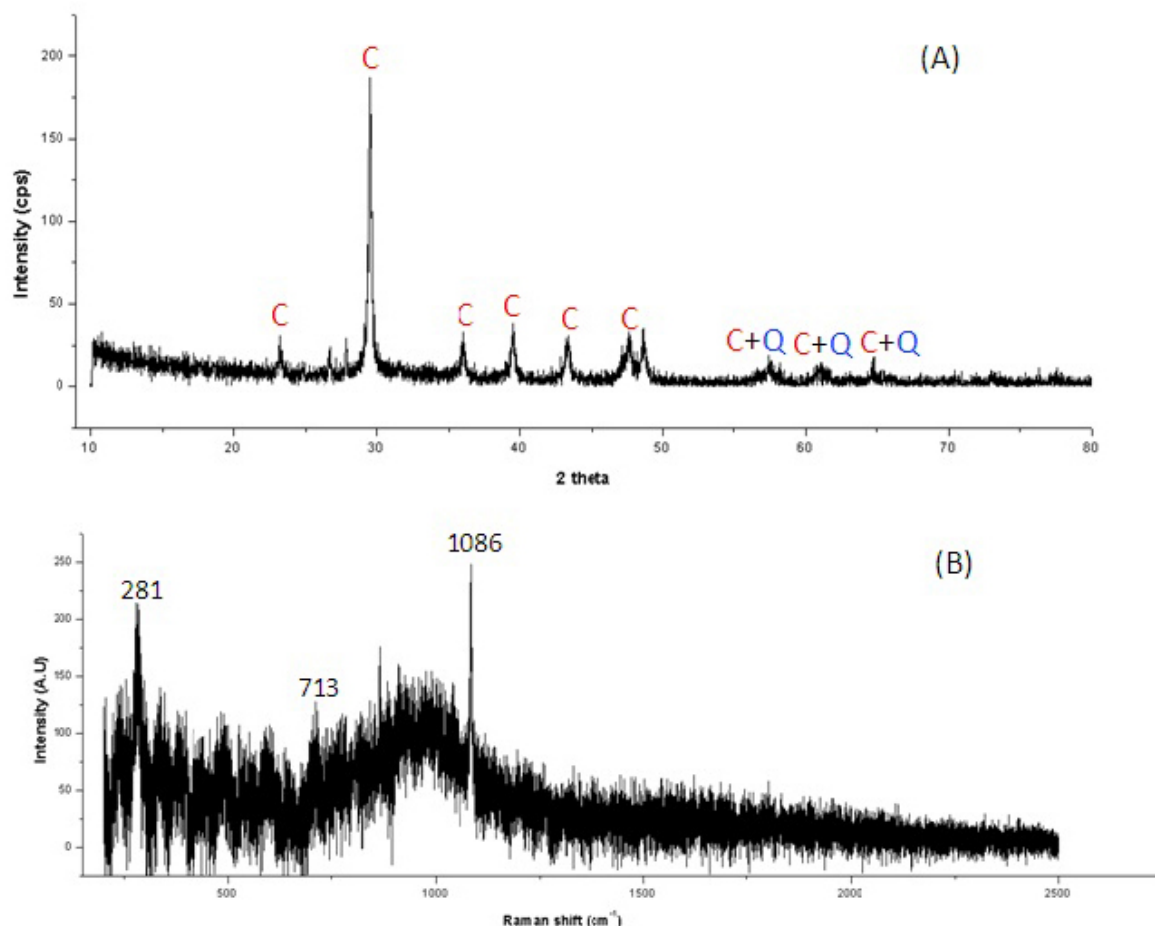
Figure 5. (A) XRD (C-calcite_ Q-quartz) & (B) Raman spectrum for RL (I) fine plaster.

pigment (Giacopetti and Satta, 2018; Parry and Coste, 1902; Sultan et al., 2017).

Furthermore, SEM images with EDX micrograph (Figure 6) of sample RP (III) detect the agglomeration of mercury and silicate confirming the pigment is a mixture of heterogeneous size particles. This also confirmed the use of natural cinnabar as red paint in the decorative wall. In the analyses of red layers, none of the samples containing the only amount of Hg and S elements were considered to be synthetic vermilion.

The physical effect of infrared is created by absorption, and mainly influences the ionic bands and dipole such as C=O, O-H, and N-H. From FTIR spectrum (Figure 7), O-H stretching and N-H stretching observed in the region between 3100-3700 cm^{-1} are due to the presence of free hydroxyl group, and C-N stretching found at 1247 cm^{-1} (Derrick et al., 2000).

The two prominent peaks of proteins were observed at 1652 cm^{-1} (amide I, C=O stretching) and 1566 cm^{-1} (amide II, C-N stretching and N-H deformation) [21]. In

addition, the most intense absorption observed, around 1739 cm^{-1}, could be assigned to the C=O bond [2]. The presence of various types of other binders could not be ruled out, since, in the sample RP (III), C-H stretching vibrations were found at 2898 cm^{-1} and 2902 cm^{-1} mainly caused by hydrocarbons i.e. RP (III) contains only this type of binders (Duran et al., 2009). Generally, the hydrocarbon stretches for unsaturated carbon groups occur at higher wavenumbers whereas saturated carbon at lower wavenumbers. Natural resins, oils, and waxes, for example, have strong hydrocarbon stretches (Derrick et al., 2000).

For detecting cadmium sulfide (Figure 8), only two peaks found at 619 cm-1 due to S-S bond in the sample RP(I) and 418 cm^{-1} due to Cd-S bond in the sample RP (II and III). The characteristic absorption bands of hematite could not be found at 470 and 535 cm^{-1}, but other than that calcite band at 871 cm^{-1} and silicates at 1051 cm^{-1} were assigned (Fiedler and Bayard, n.d.).
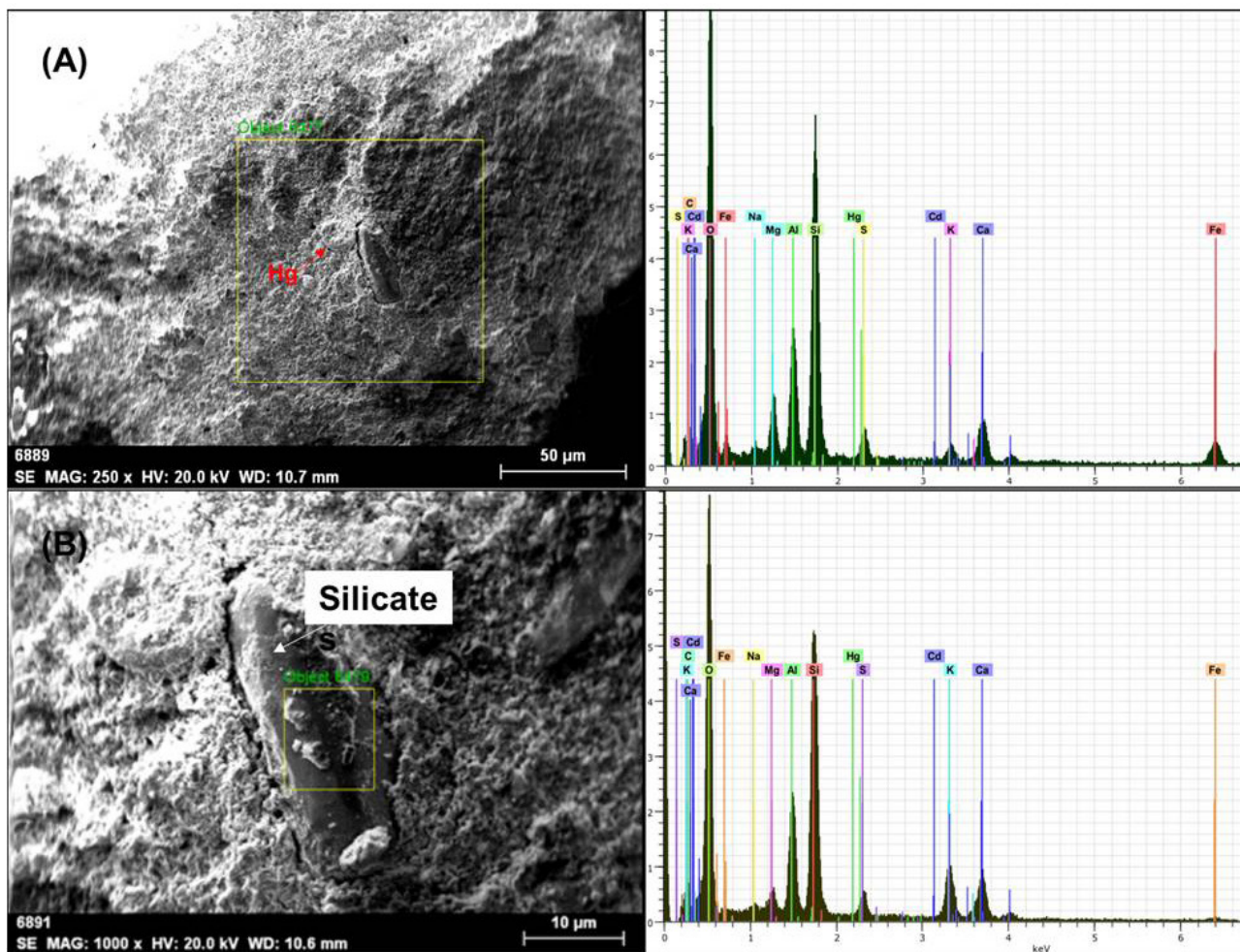
Hematite was detected by Raman analysis, with the

Figure 6. (A) SEM images of for RP (1) showing mercury and silicates as agglomeration in paint layers with (B)EDX micrograph.

main peaks found at 225, 401 (very strong), 491, 1308 and 1571 cm^{-1} (Mateos et al., 2015). Raman peaks for mercury sulfide observed at 253 and 343 cm^{-1} (Bakiler et al., 2016) while cadmium sulfide at 153 cm^{-1} (Fiedler and Bayard, n.d.). The other bands in the spectrum (particularly those at 410, 907 and 1317 cm^{-1}, some of which were overlapped with others) allow us to confirm the presence of calcite and silicates in the red pigment layers (Mateos et al., 2015).

XRD analysis (Figure 9) showed cinnabar as the main phase with the hematite and cadmium sulfide in all three samples (Bakiler et al., 2016; Fiedler and Bayard, n.d.; Gettens et al., 1993). Mineral identification was achieved by detecting a series of peaks with characteristic d values (Derrick et al., 2000; Duran et al., 2009; Hradil et al., 2011).

The portable Raman results best agree and complement the results obtained by SEM-EDX, XRD, and FTIR.

Green colored paint layer

From results show that the green colored pigment is composed of silicates with an important concentration of calcium, iron, magnesium, aluminum, and potassium (Table 2).

FTIR spectrum in the Figure 10 (B) region from 3300 to 3700 cm^{-1}, three narrow and intense bands, characteristic of the stretching vibrations of the hydroxyl groups, at 3398, 3556, and 3604 cm^{-1} are observed, strictly dependent on the nature of the octahedral cations (Aliatis et al., 2009). The OH bending modes involving the octahedral ion R^{+3} (Al) were responsible for the weak bands at 454 and 671 (Si–O–R^{+3}and R–O–H vibration). These sharp and distinct bands are suggesting quite ordered crystalline green earth specifically to celadonite (Darchuk et al., 2010).

In the region 950-1110 cm^{-1}, only 1166.23 cm^{-1} (Si–O vibration perpendicular to SiO$_4$ tetrahedral sheet) was observed while no other peak of in-plane Si–O stretching
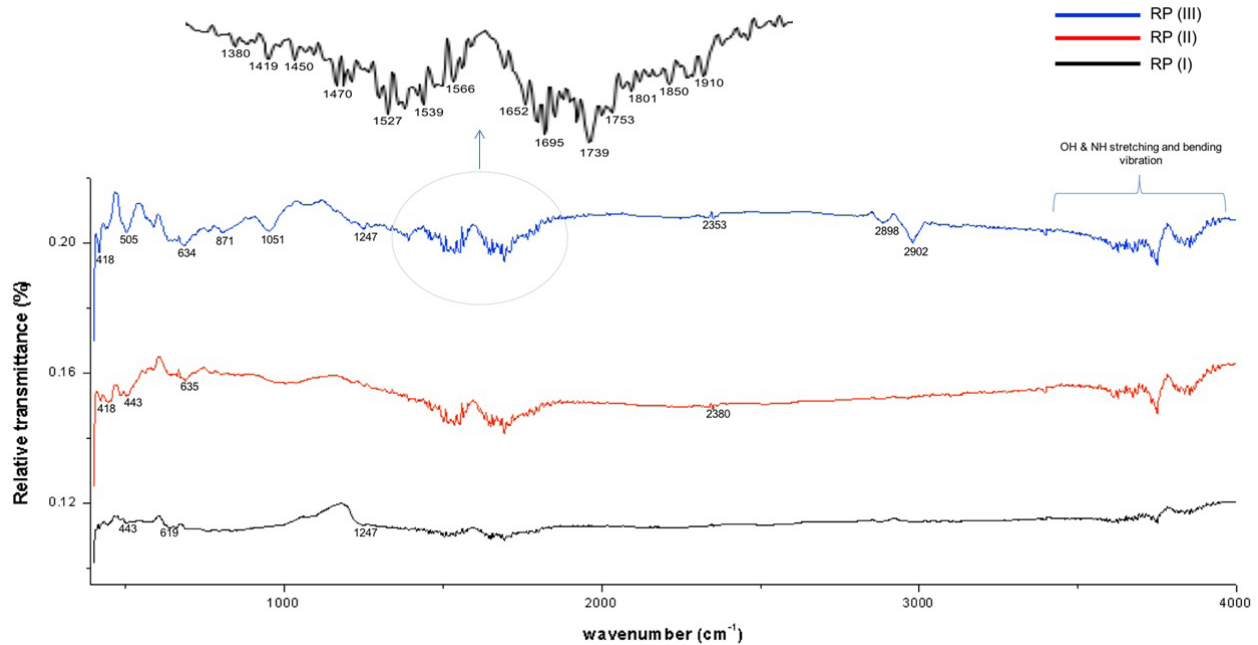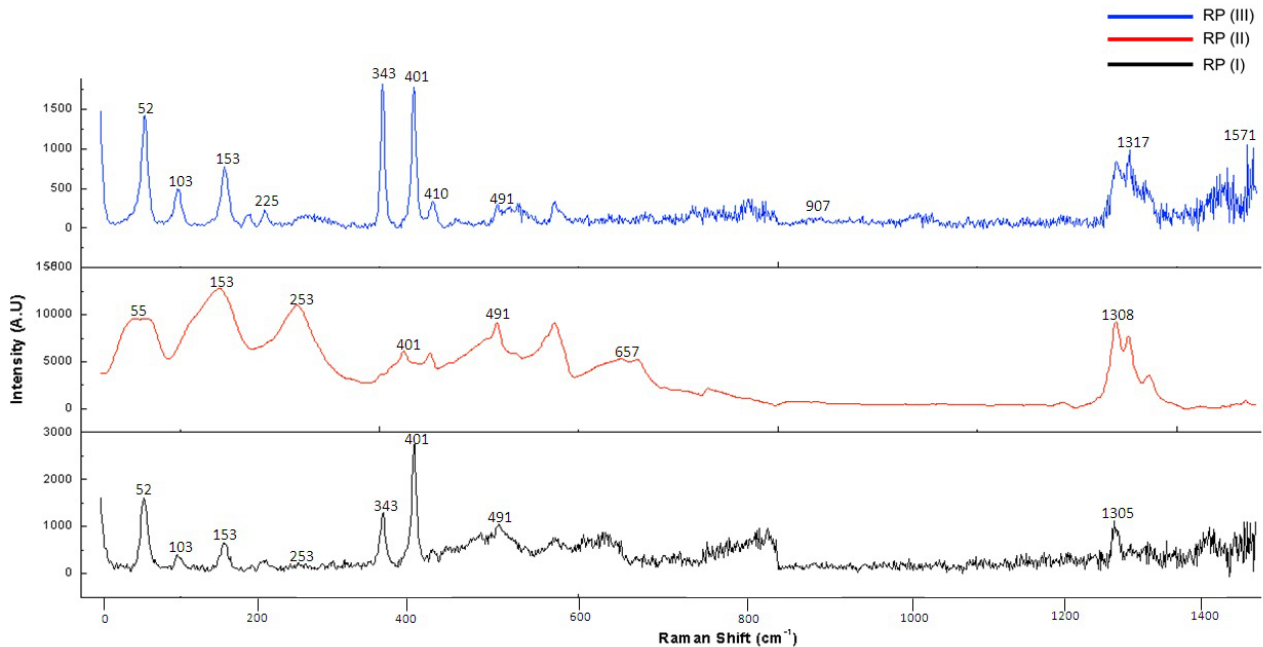
Figure 7. FTIR spectra for the red zone in specimen 1.

Figure 8. Raman spectra for the red zone in specimen 1.

modes detected (Aliatis et al., 2009). The bands at 2879 cm^{-1} (νasym and νsym CH_2), probably due to the presence of hydrocarbons and at 1498, 1627 and 1778 fatty acids were observed (Derrick et al., 2000).

Raman spectrum [Figure 10(C)] clearly shows typical peaks of calcite (152 cm^{-1} and 1086 cm^{-1}), probably due to lime present in the wall base layer. In addition, a sharp peak at 203 cm^{-1} and 390 cm^{-1} with the low-intensity peak at 278 cm^{-1} and 378 cm^{-1} is observed suggesting quite ordered crystalline structure of celadonite (Aliatis et al.,
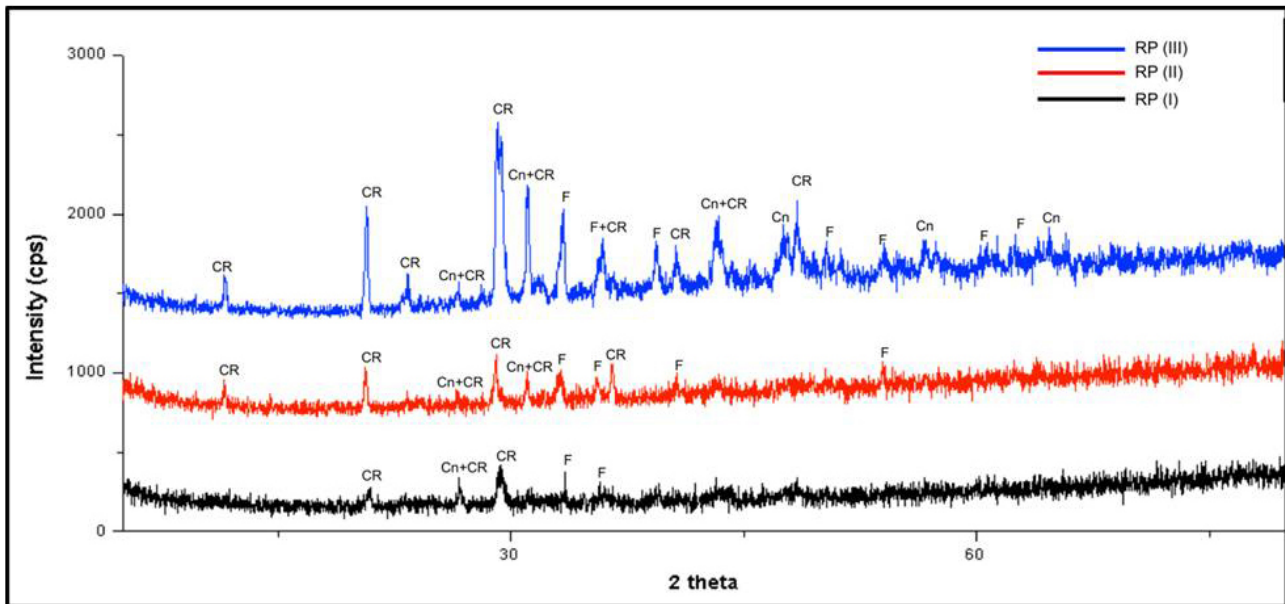
Figure 9. XRD (Cn-cinnabar_ CR-cadmium sulfide_ F-hematite) for the red zone in specimen 1.
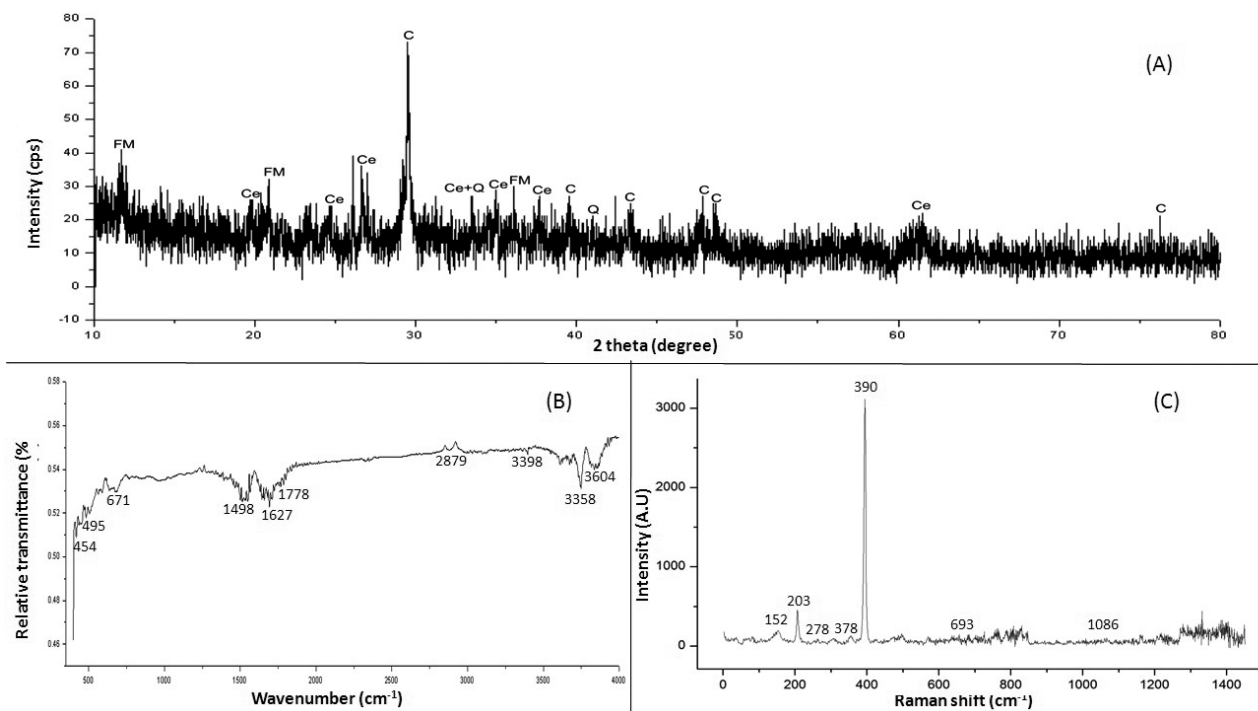

Figure 10. (A) XRD (FM-Iron mica_ Ce-celadonite_ C-calcite_ Q-quartz) (B) FTIR and (C) Raman spectrum for the green zone in specimen 2.

2009; Crupi et al., 2018).

The XRD analysis [Figure 10(A)] carried out on the surface of GP sample has indicated that it was mainly composed of calcite, quartz, iron mica and celadonite (Hradil et al., 2011).

GC-MS for analysis of binders

The samples showed the occurrence of fats, oils, and waxes (Table 3). The presence of saturated fatty acids (lauric acid, myristic acid, palmitic acid, and stearic acid) and unsaturated fatty acid (oleic acid) are typical an

Table 3. GCMS Report of binders present in RP(III) and GP samples.

Sample name	Saturated and unsaturated fatty acid	Fatty acids ester	Fatty alcohol	Alkane hydrocarbon
RP(III)	Lauric acid[1*]	Ethyl pentadecanoate[6]		
	Myristic acid[2]	Ethyl heptadecanoate[7]		
	Palmitic acid[3]	Oleic acid propyl ester[8]		
	Oleic acid[4]	Behenylbehenate[9]		
	Stearic acid[5]			
GP	Lauric acid[10]	Ethyl palmitate[12]	Lauryl alcohol[13]	Tetrakosane[15]
	Capric acid[11]		Myristyl alcohol[14]	Heneicosane[16]

*Chromatogram showing peak from 1-16 as superscript corresponding to the detected compound.

example of drying oils which can be derived from either plant, mineral and animal fats (Masschelein-Kleiner, 1985).

Fatty acids ester, fatty alcohol (cerides) and saturated hydrocarbons also detected in some samples are the components of waxes that melt easily and are difficult to saponify using alkalis. From the FTIR analysis, evidence for the presence of an amino group was determined, but nothing was found by GC-MS spectra of any sample. It may also be possible that free amino acids and fatty acids present in the sample were converted to ester followed by derivatization (Bonaduce et al., 2009; Marcaida et al., 2018).

GCMS procedure has not claimed for any calculation on acid index and iodine index. These explanations exclusively based on interpreting data of observed peaks (Figure 11).

Sometimes, pigments impede the drying process in the different oils such as oleic acid (unsaturated fatty acids) oxidize to become a film by forming cross-links that protect the paint from deterioration. The drying power of unsaturated oils is directly proportional to the concentration of C=C double bonds enable oxidation and polymerization reactions which support the formation of the film (Masschelein-Kleiner, 1985). That film on the paint surface was not detected in any sample.

DISCUSSION

The analytical studies show that the decorative wall at Chatta Chowk mainly composed of a thin pigment layer and a fine lime layer over the rough plaster layer. In both specimens, the paint layer indicates that each layer was applied sequentially in a well-controlled manner; a new layer is added only after the previous layer was dry. The combination of layers explains the secco technique used in the decorative works of Chatta Chowk. Generally, secco paintings are fragile and weakly bonded to the fine plaster when compared to the fresco paintings (Demir et al., 2018). There were micro-cracks and detachment of the binding layer on the paint surface from the fine plasters layer observed. The supported rough plaster has been the widespread loss from primary support. The loss may be associated with mechanical action, water infiltration and possibly the inherent susceptibility of the plaster. Therefore, the present condition of decorative plaster requires a comprehensive effort for their conservation.

Three red pigments layers were found a mixture of red ochre (Fe_2O_3), cinnabar (HgS), cadmium sulfide and clay minerals. When comparing the colors in the specimen 1, it must be pointed out that the pigments were blended to accomplish specific hue and the craftsmen varied the pigment particle and pigment to binder ratio to accomplish tonal variation and another surface impact. The high amount of mercury shows the primary color and the other two metal cadmium and iron were incorporated to change the hue of color. However, there was no significant change in color was observed for second and third pigment layers. Mercury sulfide is found in nature as the mineral cinnabar, or it can be obtained through wet or dry methods as artificial vermilion (Franquelo and Perez-Rodriguez, 2016; Marcaida et al., 2018). Distinguishing cinnabar from artificial vermilion is challenging, although cinnabar may sometimes be identified through the heterogeneous sized, irregular shaped and thick pigment particles. The agglomeration of mercury and silicate conformed that the pigment is natural rather than the synthetic one.

The green colored pigment contains silicates, calcium, iron, magnesium, aluminum, and potassium; an absence of
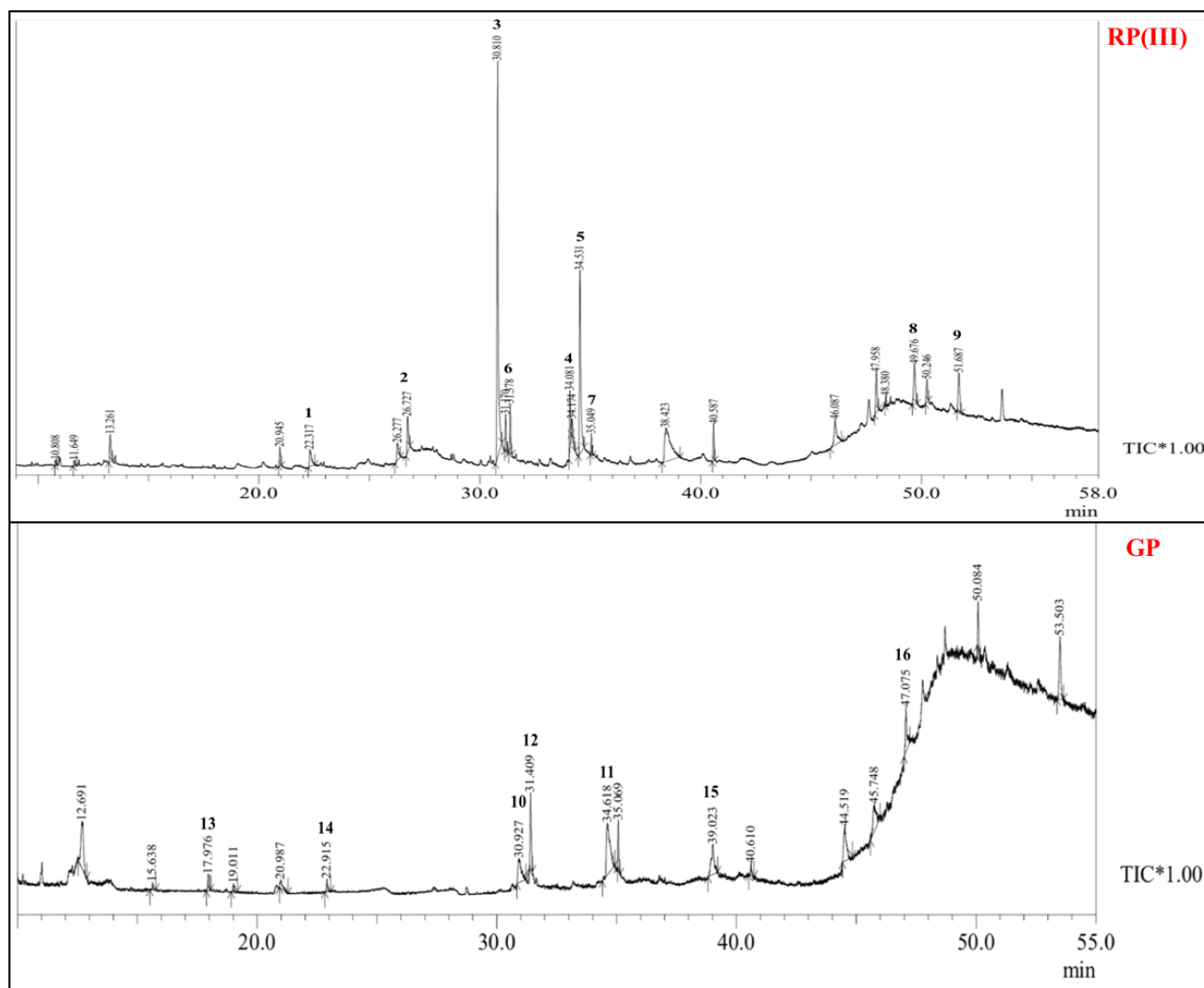
PM

Figure 11. GC-MS analysis showing total ion chromatogram of sample RP(III) and GP sample.

copper excludes the existence of malachite or atacamite. The higher amounts of magnesium and calcium due to a carbonated lime binder and lower amounts of iron, aluminum, and silicon in the green pigment suggested that the predominant color in the decorative wall is green earth. The primary source minerals for this pigment known as green earth are the celadonite, glauconite and dioctahedral micas (Hradil et al., 2011). Furthermore, a lesser amount of zinc and chromium from SEM-EDX data may be related to either different factors or considered as impurities, often found to be mixed together with the green earth in the decorative wall. However, the presence of these metal-related minerals was not found in XRD and Raman analyses.

When the results are considered as a whole, it can be said that the green earth derived from celadonite

$K[(Al,Fe^{3+}),(Fe^{2+},Mg)](AlSi_3,Si_4)O_{10}(OH)_2$ with low aluminum content and a very small replacement of Al for Si in the tetrahedral layer evidencing the trend Si>Mg>Al.

The presence of high quantities of salts of fatty acids and hydrocarbons, together with the detection of ketones, lead us to suspect the possibility that vegetable compounds and wax may be present as organic binders. The use of binders could be varied depends on sources as verified by FTIR and GC-MS analyses. From the GC-MS analyses of all the paint layers, fats, oils, and waxes as organic materials were detected. Hence, it can be said that organic materials were used in the preparation of paint layers.

CONCLUSION

Mineralogical characteristics of the Chatta Chowk decorative wall in the Red Fort at Delhi (India) were

investigated by using XRD, FT-IR spectroscopy, Raman, SEM-EDS and GC-MS analysis. The work supports useful information to enlarge the knowledge of the decorative wall executed in Chatta Chowk. The results of the analysis indicated that wall paintings were executed in a secco technique with the help of a binder on dry fine plasters. The three-layered structure of specimen 1 showed that the first plaster layer constructed over the second and third pigment layer because of hiding the previously damaged layers. Although the variation of color was observed between the first two layers but failed to explain the structure of the decorative wall. In the execution of paintings, cadmium sulfide, cinnabar and, red ochre for red pigments and celadonite for green pigment were used in artworks. Combination of cadmium sulfide, mercury sulfide, and red ochre pigments have not been reported earlier in India, this study allows us to understand the extensively used mercury with iron and cadmium. It is well known from data, there was considerable use of mercury in the preparation of red paints, and either exists in Mughal times or may be imported from other countries such as Rome and China. S. R. N. Murthy mentioned in his paper about an occurrence of mercury near the river Nagamandala and great mountain Kardama, containing four substances: cinnabar, orpiment, sulfur, and realgar, which are in existence from ancient times(Murthy, 1978). The technical examination of these specimens has helped in the future for the conservation and restoration of decorative walls.

REFERENCES

Agrawal O.P. and Pathak R., 2001. Examination and conservation of wall paintings-a manual.

Aliatis I., Bersani D., Campani E., Casoli A., Lottici P.P., Mantovan S., Marino I.-G., Ospitali F., 2009. Green pigments of the Pompeian artists' palette. Spectrochimica Acta Part A: Molecular and Biomolecular Spectroscopy 73, 532-538.

Bakiler M., Kırmızı B., Öztürk Ö.O., Hanyalı Ö.B., Dağ E., Çağlar E., Köroğlu G., 2016. Material characterization of the Late Roman wall painting samples from Sinop Balatlar Church Complex in the black sea region of Turkey. Microchemical Journal 126, 263-273.

Bonaduce I., Cito M., Colombini M.P., 2009. The development of a gas chromatographic-mass spectrometric analytical procedure for the determination of lipids, proteins and resins in the same paint micro-sample avoiding interferences from inorganic media. Journal of Chromatography A 1216, 5931-5939. https://doi.org/https://doi.org/10.1016/j.chroma.2009.06.033.

Caner E., 2003. Archaeometrical investigation of some seljuk plasters. The Middle East Technical University.

Crupi V., Fazio B., Fiocco G., Galli G., La Russa M.F., Licchelli M., Majolino D., Malagodi M., Ricca M., Ruffolo S.A., 2018. Multi-analytical study of Roman frescoes from Villa dei Quintili (Rome, Italy). Journal of Archaeological Science: Reports 21, 422-432.

Darchuk L., Tsybrii Z., Worobiec A., Vázquez C., Palacios O.M., Stefaniak E.A., Rotondo G.G., Sizov F., Van Grieken R., 2010. Argentinean prehistoric pigments' study by combined SEM/EDX and molecular spectroscopy. Spectrochimica Acta Part A: Molecular and Biomolecular Spectroscopy 75, 1398-1402.

Demir S., Şerifaki K., Böke H., 2018. Execution technique and pigment characteristics of Byzantine wall paintings of Anaia Church in Western Anatolia. Journal of Archaeological Science: Reports 17, 39-46.

Derrick M.R., Stulik D., Landry J.M., 2000. Spectral Interpretation. In Infrared spectroscopy in conservation science, pp. 182-125. Getty Publications.

Duran A., De Haro M.C., Pérez-Rodríguez J.L., Franquelo M.K., Herrera L., Justo A., 2009. Determination of pigments and binders in Pompeian Wall paintings using synchrotron radiation - high-resolution X-Ray powder diffraction and conventional spectroscopy - chromatography. Archaeometry 52, 286-307.

Fiedler I. and Bayard M. (n.d.). Cadmium Yellows, Oranges, and Reds. In R. L. Feller (Ed.), Artist's Pigments, pp. 65-104. Archetype Publications.

Franquelo M.L. and Perez-Rodriguez J.L., 2016. A new approach to the determination of the synthetic or natural origin of red pigments through spectroscopic analysis. Spectrochimica Acta Part A: Molecular and Biomolecular Spectroscopy 166, 103-111.

Gettens R.J., Feller R.L., Chase W.T., 1993. Vermilion and Cinnabar. In A. Roy (Ed.), Artist's' Pigments, pp. 159-177. Archetype Publications Ltd.

Giacopetti L. and Satta A., 2018. Reactivity of Cd-yellow pigments: role of surface defects. Microchemical Journal 137, 502-508.

Hradil D., Píšková A., Hradilová J., Bezdička P., Lehrberger G., Gerzer S., 2011. Mineralogy of Bohemian green earth pigment and its microanalytical evidence in historical paintings. Archaeometry 53, 563-586.

Janssens K., Van der Snickt G., Vanmeert F., Legrand S., Nuyts G., Alfeld M., Monico L., Anaf W., De Nolf W., Vermeulen M., 2017. Non-invasive and non-destructive examination of

artistic pigments, paints, and paintings by means of X-ray methods. In Analytical Chemistry for Cultural Heritage, pp. 77-128. Springer.

Karimy A.-H. and Holakooei P., 2015. Analytical studies leading to the identification of the pigments used in the Pīr-i Hamza Sabzpūsh Tomb in Abarqū, Iran: a reappraisal. Periodico Di Mineralogia, 84.

Marcaida I., Maguregui M., Morillas H., Prieto-Taboada N., de Vallejuelo S.F.-O., Veneranda M., Madariaga J.M., Martellone A., De Nigris B., Osanna M., 2018. In situ non-invasive characterization of the composition of Pompeian pigments preserved in their original bowls. Microchemical Journal 139, 458-466.

Masschelein-Kleiner L., 1985. Description of the main Natural film-forming materials. In Ancient binding media, varnishes and adhesives, pp. 33-39.

Mateos L.D., Cosano D., Mora M., Muñiz I., Carmona R., Jiménez-Sanchidrián C., Ruiz J.R., 2015. Raman microspectroscopic analysis of decorative pigments from the Roman villa of El Ruedo (Almedinilla, Spain). Spectrochimica Acta Part A: Molecular and Biomolecular Spectroscopy 151, 16-21.

Murthy S.R.N., 1978. An Occurrence of Cinnabar in Rasārṇavakalpa. Geological Survey of India, 14 (31st may), 83-86.

Parry E. J. and Coste J.H., 2002. The Cheimistry Of Pigments. London Scott, Greenwood & Co.

Prehistoric pigments. (n.d.). Royal Society Of Chemistry. http://www.rsc.org/learn-chemistry/content/filerepository/ CMP/00/004/139/A002 Prehistoric Pigments Version 3 PJO. pdf.

Romano F.P., Pappalardo L., Masini N., Pappalardo G., Rizzo F., 2011. The compositional and mineralogical analysis of fired pigments in Nasca pottery from Cahuachi (Peru) by the combined use of the portable PIXE-alpha and portable XRD techniques. Microchemical Journal 99, 449-453.

Rusu R.D., Simionescu B., Oancea A.V., Geba M., Stratulat L., Salajan D., Ursu L.E., Popescu M.C., Dobromir M., Murariu M., 2016. Analysis and structural characterization of pigments and materials used in Nicolae Grigorescu heritage paintings. Spectrochimica Acta Part A: Molecular and Biomolecular Spectroscopy 168, 218-229.

Sanyal S., 2008. Significance of a Mughal Mall and its role in achieving safety. Structural Analysis of Historic Construction: Preserving Safety and Significance, Two Volume Set: Proceedings of the VI International Conference on Structural Analysis of Historic Construction, SAHC08, 2-4 July 2008, Bath, United Kingdom, 1, 161.

Şerifaki K., Böke H., Yalçın Ş., İpekoğlu B., 2009. Characterization of materials used in the execution of historic oil paintings by XRD, SEM-EDS, TGA and LIBS analysis. Materials Characterization 60, 303-311.

Sultan S., Kareem K., He L., Simon S., 2017. Identification of the authenticity of pigments in ancient polychromed artworks of China. Analytical Methods 9, 814-825.